

Supporting information for

Tuning the Nanocellulose-Borate Interaction To Achieve Highly Flame Retardant Hybrid Materials

Bernd Wicklein^{*,†,#}, Darko Kocjan[‡], Federico Carosio[§], Giovanni Camino[§], Lennart Bergström^{*,†}

† Department of Materials and Environmental Chemistry, Stockholm University, Svante Arrheniusv. 16C, 106 91 Stockholm, Sweden

‡ Laboratory of Biomolecular Structure, National Institute of Chemistry, CoE ENFIST, Hajdrihova 19, 1000 Ljubljana, Slovenia

§ Dipartimento di Scienza Applicata e Tecnologia, Politecnico di Torino – Sede di Alessandria, V.le Teresa Michel, 5, 15121 Alessandria, Italy

Corresponding authors:

* B. Wicklein, E-mail: bernd@icmm.csic.es

* L. Bergström, E-mail: lennart.bergstrom@mmk.su.se

Materials and Methods

Cellulose nanofiber suspension. CNF was obtained from a defibrillation process of soft wood pulp.¹ In brief, an aqueous suspension of pulp from Norwegian spruce was subjected to a TEMPO-mediated oxidation step to render carboxylated fibres (0.6 mmol g⁻¹ charge). Subsequent mechanical disintegration using a high-pressure homogenizer equipped with a 100 µm chamber renders fully defibrillated cellulose nanofibrils. The mechanical treatment results in a highly viscous CNF dispersion with a concentration of about 1 wt% and a natural pH of 7.

Boric acid and sepiolite. Boric acid (BA) was purchased from Aldrich and dissolved in Milli-Q[®] water adjusting the pH to 7 using 1 M NaOH solution. Sepiolite clay (SEP) was purchased from Aldrich and dispersed in water.

Processing. Aqueous suspensions of CNF were mixed with BA solution and in some cases with SEP dispersion using a high-speed disperser (Ultra-Turrax, IKA, Germany). The final CNF concentration was 5 mg ml⁻¹ and the BA and SEP concentrations are given in wt% in the text. The final pH of the suspensions was adjusted to pH 7 or 10 by dropwise addition of 0.1 M NaOH. The suspensions were degassed and kept under slow stirring for 24 h prior to freeze-drying. Selected samples were subjected for 3 h to a thermal treatment under N₂ atmosphere at temperatures of 180 and 450 °C in a tube furnace (LTF, Lenton, UK).

Characterization. The starting materials CNF and SEP were characterized elsewhere.^{2,3} Freeze-dried samples were analyzed by IR spectroscopy (Varian 670-IR spectrometer and 610-IR microscope), thermogravimetric analysis (TGA) in technical air and N₂ on a TAQ500 thermogravimetric balance; CNF and CNF-BA hybrids were heated at 100°C (30 min) to constant weight before increasing the temperature (10°C min⁻¹) from 100 to 800°C, BA samples were tested without the initial isothermal. 10 mg samples were placed in open alumina pans, the experimental error was ±0.5% on weight and ±1°C on temperature. The collected data were T_{onset} 10% (temperature at 10% of weight loss), T_{max} (temperature at maximum weight loss) and the residue at 800°C. Raman spectroscopy (LabRAM HR 800, Horiba), and solid state ¹¹B MAS, ¹³C CP/MAS, and ¹H-²⁹Si CP/MAS NMR spectroscopy (Varian NMR System 600, NB HX 2.3 mm probe, spinning rate 16000Hz). ¹³C chemical shifts are referenced externally with regard to the left side peak of adamantane (38.3ppm). ¹¹B chemical shifts are referenced externally with regard to the central maximum of the H₃BO₃ peak (13.65ppm). ²⁹Si chemical shifts are referenced externally with regard to tetramethylsilane (TMS). The combustion behavior of squared samples (50x50x10 mm³) has been investigated by cone calorimetry (Fire Testing Technology, FTT) under a heat flux of 35 kW m⁻² in a horizontal configuration. Prior to the tests, all specimens were conditioned for 24 h at 23 °C and 50 %rh in a climate chamber. Four specimen of each type of sample were measured in order to ensure reproducible and significant data.

Molecular modeling. The potential energy of carboxylated glucose-borate complexes was calculated using the molecular orbital method DFT/B3LYP/6-31g.

Table S1. ^{11}B MAS NMR peak area values (in %) for unreacted boric acid BA, bis-chelate borate ester L-B-L, and mono-chelate borate ester L-B of various CNF-2.4%wtBA and CNF-11%wtBA-35%wtSEP complexes. Peak areas were derived from spectral line fitting with Lorentzian/Gaussian functions positioned at the peak maximum frequencies.

Sample	BA	L-B-L	L-B
CNF-BA-SEP ^a (pH7)	82	1	17
CNF-B-SEP ^a (pH10)	30	10	60 ^b
CNF-BA:			
As prepared	88	6	6
180 °C	84	10	5
450 °C	41	32	26

a: The boron signals of the CNF-B/BA-SEP hybrids are not influenced by the presence of sepiolite as observed in the ^{11}B MAS NMR spectra in Figure S2 and discussed in the main text of this article.

b: The signal at 2 ppm of the hybrid prepared at pH 10 may in addition to L-B also contain contribution from unreacted borate anion.

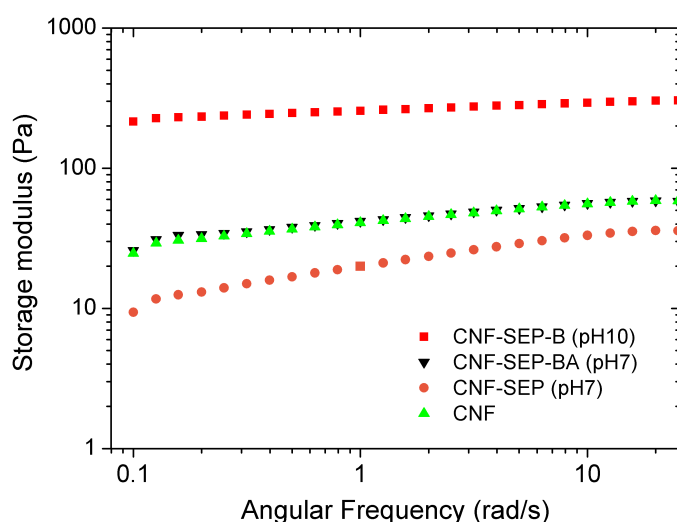


Figure S1: Storage modulus G' as function of frequency for aqueous dispersions of: CNF, CNF-35wt%SEP (pH 7), CNF-35wt%SEP-11wt%BA (pH 7), and CNF-35wt%SEP-11wt%B (pH 10). The concentration of the dispersions was 5 mg ml^{-1} .

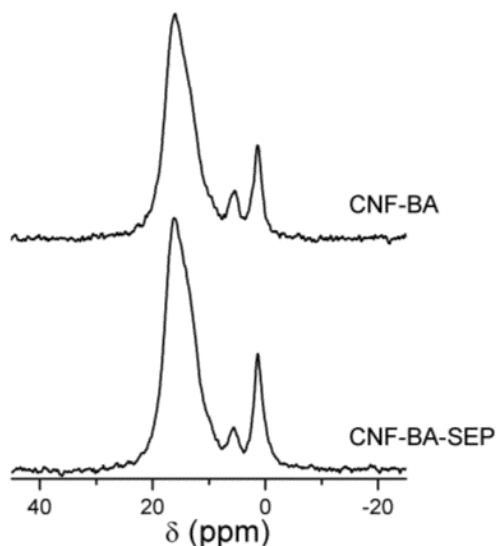


Figure S2: ^{11}B MAS NMR spectra of hybrid foams prepared at pH 7: CNF-4wt%BA and CNF-4wt%BA-14wt%SEP.

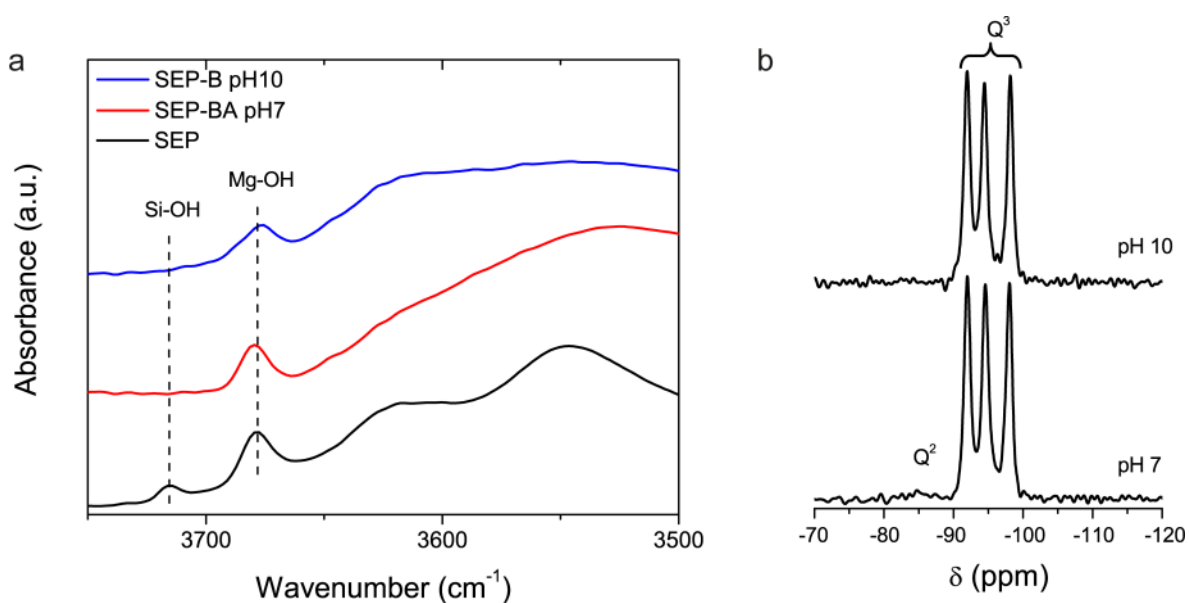


Figure S3: ATR-IR spectra of pristine sepiolite (SEP), SEP-BA (pH 7), and SEP-B (pH 10) (a). The disappearance of the Si-OH band is typically attributed to H-bonding of the silanol group and the formation of covalent bonds, in the present case of B-O-Si bonds. ^{29}Si CP/MAS NMR spectra of CNF-BA-SEP (pH 7) and CNF-B-SEP (pH 10) indicating a weak Q^2 signal attributed to geminal silanol groups on the external surface of sepiolite at pH 7 and the Q^3 signals attributed to near-edge, center, and edge silicon on the basal plane of sepiolite (b). The disappearance of the Q^2 signal is typically attributed to covalent interactions.

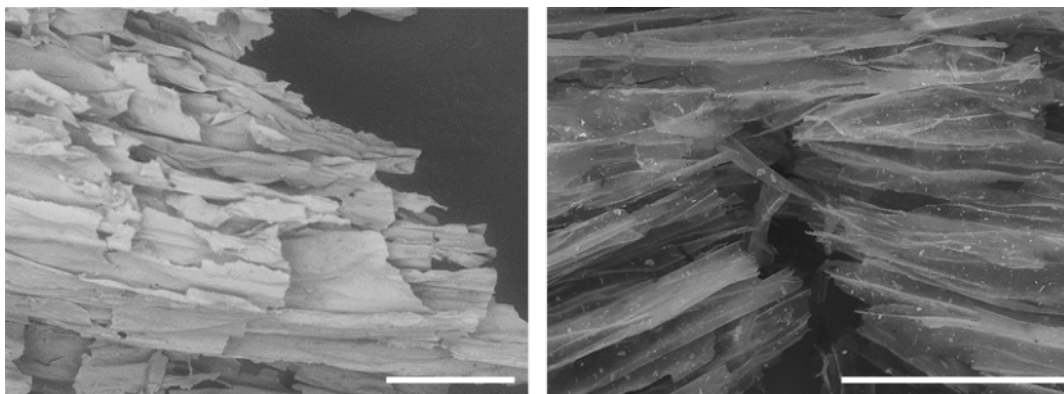


Figure S4: SEM micrographs of the CNF-11wt%B-35wt%SEP pH10 hybrid foam after cone calorimetry test. Scale bar is 500 μm .

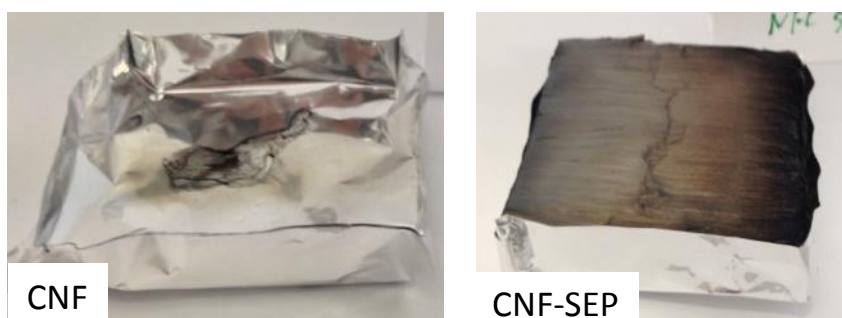


Figure S5: Photographs of residues of CNF and CNF-40wt%SEP foams after a cone calorimetry test. The respective residual weight is approx. 0 % and 44 %, respectively.

Description of molecular modeling method:

Molecular modeling methods, ab initio Hartree-Fock approximation (HF/3-21g) and a density functional approximation (DFT/B3LYP) were performed by using the software package Gaussian09.⁴

Molecular models were built by Spartan software package running on Silicon Graphics station Octane supported by IRIX OS. Molecular geometries were fully optimized with both methods, HF/3-21g and DFT/ B3LYP.

Most stable configurations of carboxylated glucose-borate complexes based on potential energy calculations were found. Both methods gave the same rank order of potential energy values for the displayed configurations.

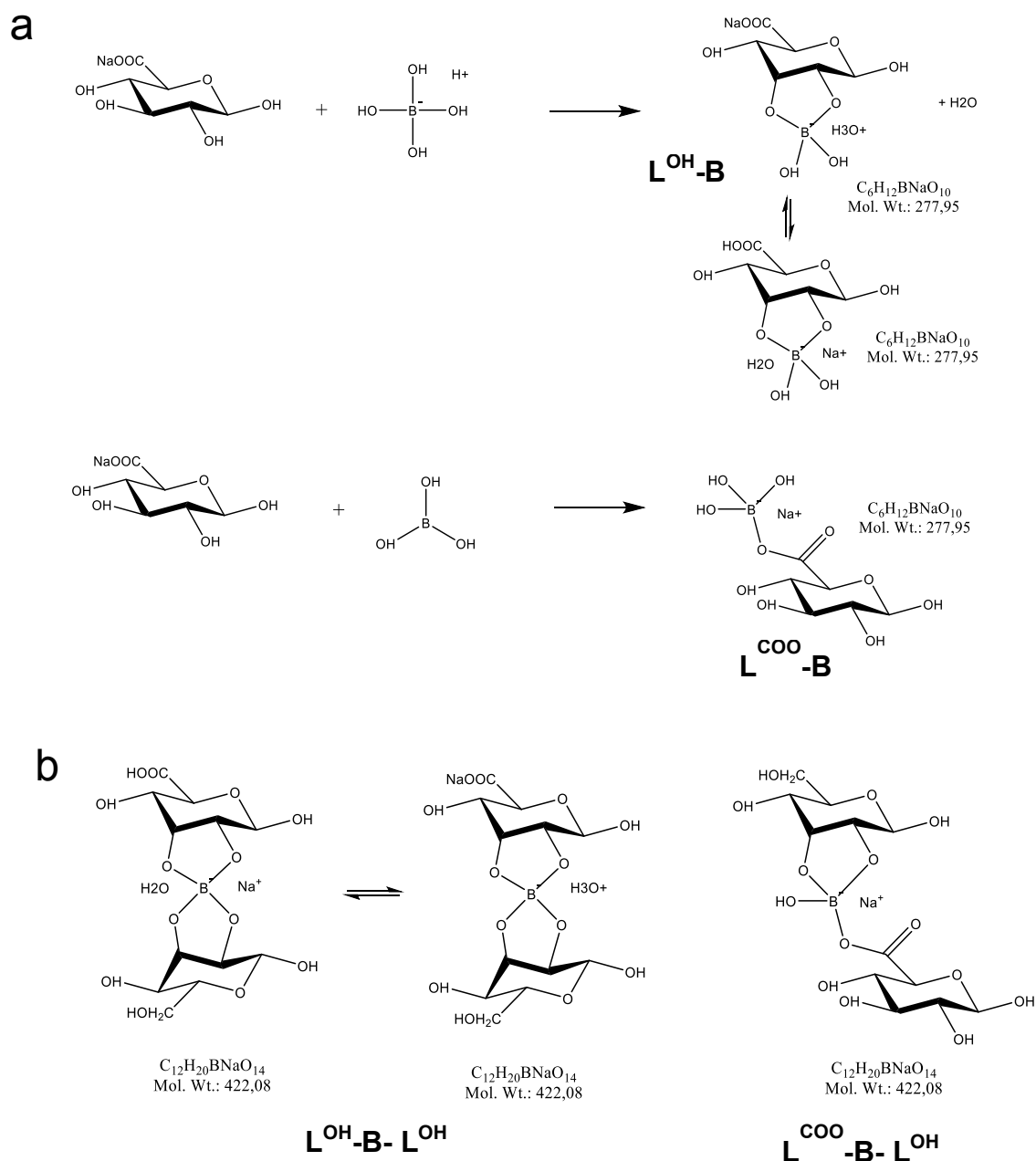


Figure S6: Most stable configurations of sodium carboxylated glucose-borate complexes based on potential energy calculations obtained with molecular modeling. The used molecular orbital methods were HF/3-21g and DFT/B3LYP/6-31g. Both methods gave similar potential energy values for the displayed configurations. In Fig. S6a are depicted the reaction of glucose with borate anion and with boric acid as supposed for pH 10 and pH 7. Fig. S6b shows the possible cross-linking of the complexes in Fig. S6a.

Table S2: Potential energy values for complexes of sodium carboxylated glucose and borate obtained from a density functional theory approximation (DFT/B3LYP) using basis set 6-31g. Energy differences between anhydride (b,d) and ester (a,c) complexes are also given. The nomenclature of the complexes refers to Figure S6.

Complex	Potential energy [a.u.]*	Energy difference [kcal/mol]
$L^{OH}-B^a$	-1175.0970535	
$L^{COO}-B^b$	-1175.1455158	-30
$L^{OH}-B-L^{OH}^c$	-1709.2242445	
$L^{COO}-B-L^{OH}^d$	-1709.2709775	-29

* a. u. = atomic units = hartree = 627.507 kcal/mol

a: $COONaGlu-B^-.H_3O^+$

b: $GluCOO-B^-.Na^+$

c: $COONaGlu-B^--Glu.H_3O^+$

d: $GluCOO-B^--Glu.Na^+$

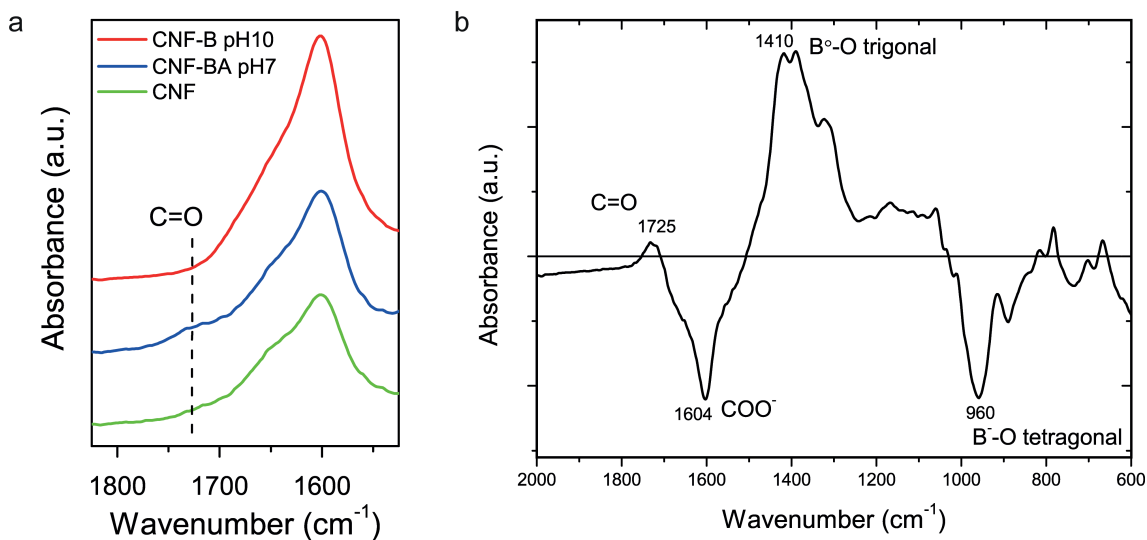


Figure S7: ATR-IR spectra of the carbonyl region of three different foams: CNF, CNF-11wt%BA pH7, and CNF-11wt%B pH10 (a). ATR-IR difference spectra between CNF-11wt%BA pH7 and CNF-11wt%B pH10 for the stretching vibrations of C=O and COO^- as well as the asymmetric B-O stretching of trigonal boron and asymmetric B-O stretching of tetragonal boron, respectively (b).

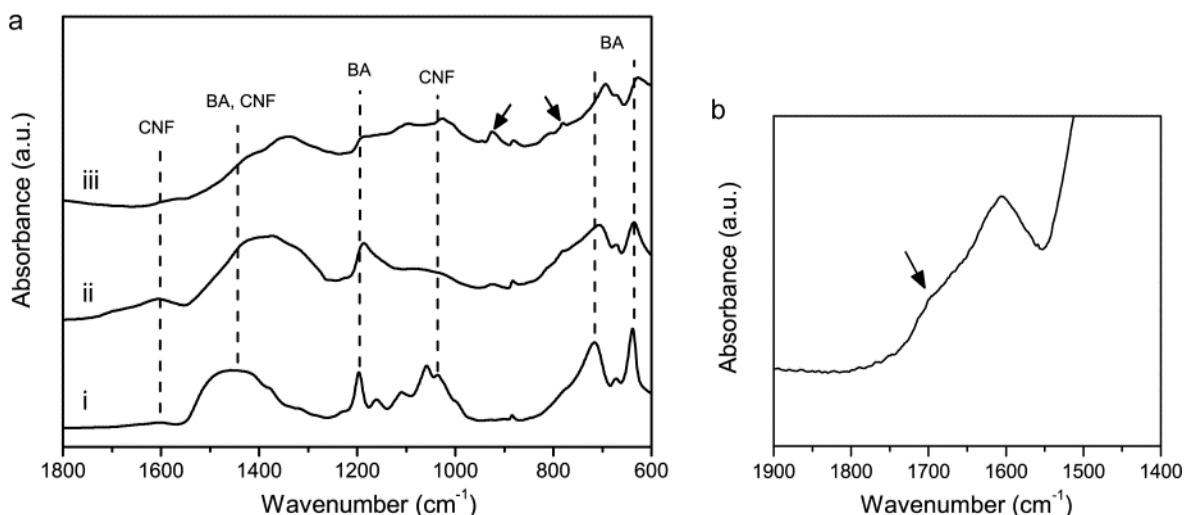


Figure S8: ATR-IR spectra of CNF-BA hybrid (60/40 w/w); as prepared at pH 7 (i); after isothermal exposure at 450 °C (ii); and 800 °C (iii) (a). Arrows in spectrum iii point out the C-H deformation and ring vibration in substituted aromatic rings. Magnification of the carbonyl range of spectrum ii, in which the arrow indicates a shoulder at 1710 cm^{-1} attributed to C=O stretching vibrations (b).

References:

- (1) Wågberg, L.; Decher, G.; Norgren, M.; Lindström, T.; Ankerfors, M.; Axnäs, K. The build-up of polyelectrolyte multilayers of microfibrillated cellulose and cationic polyelectrolytes. *Langmuir* **2008**, *24*, 784–795.
- (2) Usov, I.; Nyström, G.; Adamcik, J.; Handschin, S.; Schütz, C.; Fall, A.; Bergström, L.; Mezzenga, R. Understanding nanocellulose chirality and structure–properties relationship at the single fibril level. *Nat. Commun.* **2015**, *6*, 7564.
- (3) Ruiz-Hitzky, E. Molecular access to intracrystalline tunnels of sepiolite. *J. Mater. Chem.* **2001**, *11*, 86–91.
- (4) Gaussian 09, Revision A.02, M. J. Frisch, G. W. Trucks, H. B. Schlegel, G. E. Scuseria, M. A. Robb, J. R. Cheeseman, G. Scalmani, V. Barone, B. Mennucci, G. A. Petersson, H. Nakatsuji, M. Caricato, X. Li, H. P. Hratchian, A. F. Izmaylov, J. Bloino, G. Zheng, J. L. Sonnenberg, M. Hada, M. Ehara, K. Toyota, R. Fukuda, J. Hasegawa, M. Ishida, T. Nakajima, Y. Honda, O. Kitao, H. Nakai, T. Vreven, J. A. Montgomery, Jr., J. E. Peralta, F. Ogliaro, M. Bearpark, J. J. Heyd, E. Brothers, K. N. Kudin, V. N. Staroverov, R. Kobayashi, J. Normand, K. Raghavachari, A. Rendell, J. C. Burant, S. S. Iyengar, J. Tomasi, M. Cossi, N. Rega, J. M. Millam, M. Klene, J. E. Knox, J. B. Cross, V. Bakken, C. Adamo, J. Jaramillo, R. Gomperts, R. E. Stratmann, O. Yazyev, A. J. Austin, R. Cammi, C. Pomelli, J. W. Ochterski, R. L. Martin, K. Morokuma, V. G. Zakrzewski, G. A. Voth, P. Salvador, J. J. Dannenberg, S. Dapprich, A. D. Daniels, O. Farkas, J. B. Foresman, J. V. Ortiz, J. Cioslowski, and D. J. Fox, Gaussian, Inc., Wallingford CT, **2009**.